DOI https: //doi. org/10.1007/s11595-019-2078-y

Characterization of Metal Oxide-modified Walnut-shell Activated Carbon and Its Application for Phosphine Adsorption: Equilibrium, Regeneration, and Mechanism Studies

YU Qiongfen[1,2], LI Ming[1], NING Ping[2], YI Honghong[3,2*], TANG Xiaolong[3,2]

(1 Solar Energy Research Institute, Yunnan Normal University, Kunming 650500, China; 2 Faculty of Environmental Science and Engineering, Kunming University of Science & Technology, Kunming 650504, China; 3. School of Energy and Environmental Engineering, University of Science and Technology Beijing, Beijing 100083, China)

Abstract: We prepared a kind of metal oxide-modified walnut-shell activated carbon (MWAC) by KOH chemical activation method and used for PH_3 adsorption removal. Meanwhile, the PH_3 adsorption equilibrium was investigated experimentally and fitted by the Toth equation, and the isosteric heat of PH_3 adsorption was calculated by the Clausius-Clapeyron Equation. The exhausted MWAC was regenerated by water washing and air drying. Moreover, the properties of five different samples were characterized by N_2 adsorption isotherm, SEM/EDS, XPS, and FTIR. The results showed that the maximum PH_3 equilibrium adsorption capacity was 595.56 mg/g. The MWAC had an energetically heterogeneous surface due to values of isosteric heat of adsorption ranging from 43 to 90 kJ/mol. The regeneration method provided an effective way for both adsorption species recycling and exhausted carbon regeneration. The high removal efficiency and big equilibrium adsorption capacity for PH_3 adsorption on the MWAC were related to its large surface area and high oxidation activity in PH_3 adsorption-oxidation to H_3PO_4 and P_2O_5. Furthermore, a possible PH_3 adsorption mechanism was proposed.

Key words: phosphine; metal oxide-modified walnut-shell activated carbon; adsorption equilibrium; regeneration; mechanism

1 Introduction

Phosphine (PH_3) removal from yellow phosphorous tail gas is a compelling issue because of the resource utilization of yellow phosphorous tail gas[1-4]. Many efforts have been taken to remove PH_3 from the tail gas before it can be used as raw material gas to synthesize chemically product such as dimethylether, methyl carbonate, methanol and so on[1,5-8]. Thermal combustion[9], wet scrubbing[10,11] and gas-solid adsorption and/or catalytic oxidation[12-14] are the three common methods used for PH_3 removal from yellow phosphorous tail gas. Among these techniques, dry adsorption removal using activated carbon (AC) is a promising approach that has attracted much attention[3,5,12,15]. However, the commercially available ACs are still considered expensive due to the use of non-renewable and relatively expensive starting material such as coal. This has brought about a growing research interest in ACs production from renewable and cheaper precursors such as cherry stones, olive stones, walnut shells, paulownia wood[16-18].

Walnut-shells are considered as a good candidate for conversion to AC because of its high volatile and carbon contents, low ash content and reasonable good hardness property[6,19-21]. According to our previous work[6,22], converting walnut shells into value-added AC probably provided an effective way for both agricultural waste treatment and PH_3 adsorption removal. The effects of carbonization temperature, activation temperature, and ratio of KOH to chars on the pore development of walnut-shell activated carbons (WACs) and PH_3 adsorption performance of the metal oxide-modified walnut-shell activated carbons (MWACs) have been investigated. However, PH_3 adsorption capacity of fresh ACs is rather low[23,24]. To enhance the PH_3

(Received: Feb. 12, 2018; Accepted: Apr. 7, 2018)

YU Qiongfen (余琼粉): Assoc. Prof.; Ph D; E-mail: yqf512xpok @163.com

*Corresponding author: YI Honghong (易红宏): Prof.; Ph D; E-mail: yhhtxl@126.com

Funded by the National Natural Science Foundation of China (51566017)

adsorption capacity, a detailed importance about metal oxidative modification for PH_3 adsorption removal has been already introduced[7,25,26,3,15]. However, knowledge about adsorption equilibrium and heat of adsorption is essential for proper design and operation of gas-phase adsorption process. The regeneration performance and adsorption equilibrium of the proposed adsorbent also play an important role in PH_3 adsorption removal from yellow phosphorus tail gas.

In this research, PH_3 adsorption isotherms over the MWAC adsorbent were measured by dynamic adsorption breakthrough curve. PH_3 adsorption thermodynamics was calculated by the Clausius-Clapeyron equation. The regeneration method was also investigated. N_2 adsorption isotherm, Scanning electron microscopy/ Energy dispersive X-ray spectroscopy (SEM/EDS), X-ray photoelectron spectrometry (XPS), and Fourier transform infrared spectroscopy (FTIR) were employed to analyze the PH_3 adsorption mechanism.

2 Experimental

2.1 Preparation of MWAC

Walnut shells as the raw materials were obtained from Qujing in Yunnan province of China. The starting materials were manually chosen, cleaned with distilled water, and dried at 373 K for 24 h. The dried starting materials were crushed and sieved, and the size fraction of 0.5-1 cm was used.

WAC preparation was employed by a two-step chemical activation method including the pyrolysis carbonization of the starting materials and the KOH activation process of the resulting chars[6]. Both carbonization process and activation process were carried out in a vertical quartz reactor (700 mm length and 92 mm internal diameter), which was placed in an electrical heating furnace. The heating rate, temperature and dwell time could be programmed. Nitrogen gas (99.995% purity) at a 150 cm^3/min (STP) flow rate was used as the inert gas flushing through the reactor, right from the beginning of the pyrolysis process and activation process. In the process of pyrolysis, about 20 g of raw material were placed at the center of the reactor. The furnace temperature was increased at a rate of 10 ℃/min from room temperature to 700 ℃ and then held for 10 min. During the activation process, mixing method of the activating agent (60 g) and the resulting chars (20 g) was physical mixing. It should be emphasized that the process was done in the absence of water. KOH pellets were mechanically mixed with the chars from the carbonization process in a porcelain mortar. The resulting samples were then placed in the same furnace which was used for the carbonization process, and heated at a rate of 10 ℃/min to 700 ℃ and then held for 60 min. The resulting products after activation were thoroughly washed with 0.1 mol/L hydrochloric acid followed by hot distilled water to remove the residual KOH until the pH value of the washed solution ranged from 6.5 to 7.0.

Moreover, the MWAC adsorbent was prepared by impregnation of the WAC with an aqueous solution of the precursors ($Cu(NO_3)_2{\cdot}3H_2O$, $Zn(NO_3)_2{\cdot}6H_2O$, and $La(NO_3)_3{\cdot}nH_2O$) in the appropriate concentrations to obtain proper metal mass loadings[15]. The mass loadings for Cu, Zn, and La were 2.5%, 0.167%, and 0.0833%, respectively. During the impregnation, a beaker that contained both the WAC and active components aqueous solution were put in an ultrasonic laboratory cleaner operating at a frequency of 40 kHz with an instrument power of 300 W, and this ultrasonic-assisted impregnation process continued for 40 min at 30 ℃. These wet samples were dried in a drying cabinet at 110 ℃ for 12 h followed by calcining in a furnace at 350 ℃ for 6 h.

2.2 PH_3 adsorption of MWAC

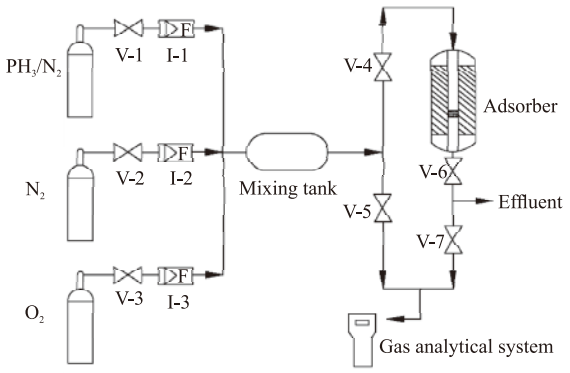

Fig.1 Schematic diagram of PH_3 adsorption experimental system

The schematic diagram of PH_3 adsorption experimental system is given in Fig.1. Adsorption isotherm measurements were made by a dynamic method using a step change in concentration[27]. Before the adsorption experiment, each sample (0.6 g) was treated firstly at 393 K for 60 min in N_2 and then cooled to appropriate temperature. Subsequently, the N_2 flow was switched to a mixed gas for PH_3 adsorption. The PH_3 concentration was measured by C16 portable gas detector (supplied by Analytical Technology, Inc). The PH_3 adsorption capacity was calculated using

the integrated area below the adsorption removal efficiency curve, the influent PH_3 concentration, mass of carbon, and flow rate. When regeneration performance of exhausted sample was investigated, the PH_3 concentration was measured every 30 min until the removal efficiency was below 90%. The breakthrough point of the adsorbent was set at PH_3 removal efficiency of 90%. The PH_3 breakthrough capacity (q_{90}) was also calculated in the same way.

2.3 Regeneration of exhausted MWAC

After PH_3 adsorption process, attempts were made to regenerate the exhausted adsorbents by water washing and air drying. The regenerated adsorbents were used in subsequent adsorption/regeneration cycles. During regeneration process, the exhausted MWAC adsorbents were firstly washed with distilled water in order to remove adsorbed species and then dried in a drying cabinet at 393 K for 12 h. After each adsorption cycle the suffix "A" followed by the number of the cycle was added. After regeneration, the suffix "*R*" was added followed by the number consequent with the number of the adsorption run. For example, the MWAC-A1 represents the exhausted adsorbent after the first adsorption run. After the first regeneration, the sample can be designated as MWAC-R1.

2.4 Characterization of adsorbent samples

Micromeritics Tristar Ⅱ 3020 surface area and porosity analyzer was used to measure nitrogen adsorption isotherms at −77 K. The samples were initially outgassed at 473 K for 6h before adsorption isotherms. The BET surface area was calculated from the isotherms using the Brunauer-Emmett-Teller (BET) equation. The *t*-plot method was applied to calculate the micropore volume. The total pore volume was estimated to be the liquid volume of adsorbate (N_2) at a relative pressure of 0.985.

XL30ESEM-TMP (poland) type scanning electron microscope (SEM) was used for microstructure observation of the interface and element distribution of samples. The contents of metal elements were determined with EDS pattern (EDS: EDAX, PHOENIXTM, USA).

XPS (PHI 5500) analysis used Al Kα radiation with energy of Al rake and power of 200 W. Kinetic energies of the photoelectrons were measured by a two-stage spectrometer. The analyzer resolution was 1 eV. An Ar^+ ion gun was used to sputter clean specimen surfaces. The ion energy was set to 1 keV and the sputtering time was 10 min. The photoelectron spectra were calibrated using the C 1s signal detected at a binding energy of 284.8 eV from adventitious carbon.

FTIR measurements were performed on a Thermo Nicolet AVATAR FT-IR 360 instrument. Potassium bromide pellets containing 0.5% of the adsorbents were used in FTIR experiments and 34 scans were accumulated for each spectrum in transmission, at a spectral resolution of 4 cm^{-1}. The spectrum of dry KBr was taken for background subtraction.

2.5 Isosteric heat of adsorption calculation

The Clausius-Clapeyron equation and Toth equation were applied to the isotherm data to calculate the isosteric heat of adsorption (ΔH_s).

The Clausius-Clapeyron equation is as follows:

$$\Delta H_S = RT^2\left(\frac{\partial \ln C}{\partial T}\right) \tag{1}$$

where, ΔH_s is the isosteric heat of adsorption (J/mol), R is the ideal gas constant (8.314 J/(mol·K)), T is the adsorption temperature (K), and C is the adsorbate gas concentration at equilibrium (mg/m^3).

The Toth euqation is as follows:

$$q = \frac{q_m bC}{(1+(bC)^n)^{1/n}} \tag{2}$$

where, q is the adsorbed amount per unit weight of adsorbent (mg/g), q_m, b, and n are the Toth equation parameters.

3 Results and discussion

3.1 PH_3 adsorption isotherms analysis

PH3 adsorption isotherms on the MWAC adsorbent at 333-363 K and fitting results are shown in Fig.2. The fitting parameters and correlation coefficient (R^2) are summarized in Table 1.

As shown in Fig.2 the PH_3 equilibrium adsorption amount increases rapidly when the adsorption temperature increases from 333 K to 343 K, but the equilibrium capacity decreases with the increasing of adsorption temperature from 343 K to 363 K. Therefore, when the adsorption temperature ranged from 333 K to 363 K, the optimal adsorption temperature was 343 K and the maximum equilibrium adsorption amount was 595.56 mg/g at 343 K. This reason may be that PH_3 adsorption on the MWAC adsorbent is mainly an exothermic chemisorption process. Firstly, possibility and amount of activated PH_3 increase with the increasing of adsorption temperature because of the chemisorption process. Secondly, increasing adsorption temperature is not favorable to cause the

equilibrium shift to the adsorption side because of the exothermic adsorption process. Therefore, there is an optimal adsorption temperature of 343 K during the experimental temperature range.

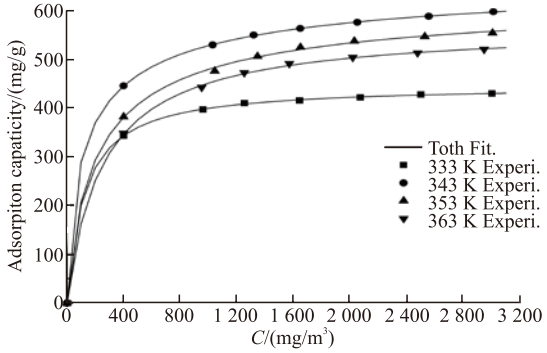

Fig.2 Experimental adsorption isotherms and fitting results at different temperatures. Experimental conditions: adsorbent amount = 0.6 g, O_2 =0.5%, N_2 = the balance, and GHSV = 21000 h^{-1}

Table 1 Adsorption isotherm parameters fitted by the Toth equation

T/K	q_m/(mg/g)	b/(m^3/mg)	n	R^2
333	444.82	0.0079	1.0250	0.9999
343	686.22	0.0191	0.5973	0.9999
353	633.52	0.0070	0.7458	0.9996
363	567.38	0.0041	0.9727	0.9998

According to Fig.2 and Table 1, the fitting results of the Toth Equation are in good agreement with experimental data and all correlation coefficients are greater than 0.9995. Compared with other three temperatures, the biggest amount of equilibrium adsorption was 686.22 mg/g at 343 K.

3.2 PH_3 adsorption thermodynamics

The isosteric heats of adsorption are shown in Fig.3. The isosteric heat of adsorption decreases with the increasing of PH_3 adsorption amounts on the MWAC adsorbent. The isosteric heat of adsorption was 80.64 kJ/mol when the PH_3 adsorption amount was 20 mg/g. However, when the PH_3 adsorption amount increased to 400 mg/g, the isosteric heat of adsorption decreased to 44.17 kJ/mol. As stated by Hill[28], if different levels of surface energy exist and the interactions between adsorbed molecules can not be neglected, the isosteric heat of adsorption varies with the surface coverage. Therefore, it can be concluded that the MWAC adsorbent has an energetically heterogeneous surface.

The negative value of isosteric heat of adsorption is equal to enthalpy changes during the adsorption process. PH_3 adsorption on MWAC adsorbent is an exothermic process because the enthalpy changes are negative during the adsorption process. Considering that values of isosteric heat of adsorption range from 43 kJ/mol to 90 kJ/mol, PH_3 adsorption process may be a dominant of chemical adsorption. The adsorption species of PH_3 chemical adsorption will be analyzed in the latter study of PH_3 adsorption mechanism.

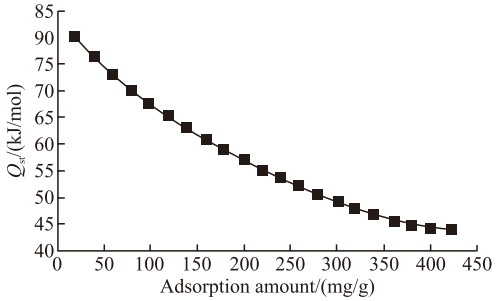

Fig.3 Isosteric heat of adsorption on the MWAC

3.3 Regeneration performance of exhausted MWAC

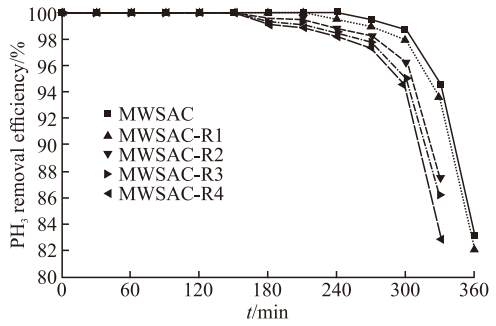

Fig.4 PH_3 adsorption removal efficiency over the MWACs after subsequent adsorption/regeneration cycles. Experimental conditions: T=343 K, PH_3=872ppm, O_2=1%, N_2 = the balance, and GHSV=10 500 h^{-1}

After PH_3 adsorption, the exhausted sorbents were regenerated by water washing and air drying. PH_3 removal efficiencies on the MWAC adsorbents after subsequent adsorption/regeneration cycles are shown in Fig.4. PH_3 breakthrough adsorption capacities for MWAC, MWAC-R1, MWAC-R2, MWAC-R3, and MWAC-R4 are 296.33, 295.61, 269.39, 268.88, and 268.58 mg/g, respectively. Except for MWAC and MWAC-R1 adsorbents, there was only a little adsorption difference among the other three regenerated samples. Moreover, the regeneration method showed that the adsorbents could be regenerated to about 91% of the initial breakthrough adsorption capacity and time. The results revealed that PH_3 adsorption performances of MWAC-R adsorbents owned good stability. Wang *et al*[5] and Yi *et al*[15] found that PH_3 adsorbed on the modified activated carbon could be oxidized to form H_3PO_4 and P_2O_5, which were removed easily from the

modified carbon surface when using water washing regeneration. Therefore, this regeneration method using water washing and air drying provides an effective way for both adsorption species recycling and regeneration of exhausted carbons. The result confirms that the MWAC adsorbents will be one of the candidates for both PH_3 adsorption removal and recycling from yellow phosphorus tail gas.

3.4 PH_3 adsorption mechanism

In order to analyze PH_3 adsorption mechanism on the MWAC adsorbent, WAC, MWAC, MWAC-AB, MWAC-AQ, and MWAC-R5 were characterized by N_2 adsorption isotherm, SEM/EDS, XPS, and FTIR analysis. WAC and MWAC represent the walnut-shell activated carbon before and after modification, respectively. The MWAC-AB and MWAC-AQ samples represent MWAC adsorbent after adsorption breakthrough process and adsorption equilibrium, respectively. After undergoing five adsorption-regeneration cycles, the sample was designated as MWAC-R5.

3.4.1 N_2 adsorption isotherm analysis

Table 2 N_2 adsorption isotherm characterizations of five different samples

Samples	S_{BET} /(m^2/g)	V_{total} /(cm^3/g)	V_{mic} /(cm^3/g)	V_{mic}/V_{total} /%	D_a /nm
WASC	1636	0.782	0.641	81.97	1.913
MWAC	1419	0.696	0.544	78.16	1.962
MWAC-AB	90	0.0514	0.0259	50.39	2.298
MWAC-AQ	2	0.00524	0	0	10.274
MWAC-R5	1385	0.680	0.539	79.26	1.963

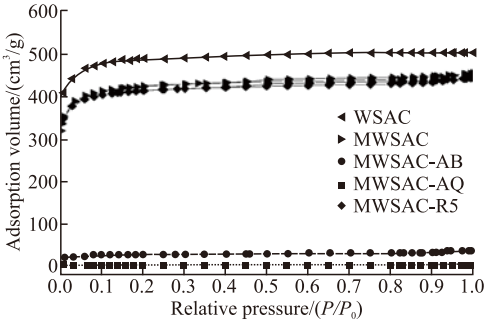

Fig.5 N_2 adsorption isotherms of five different samples

N_2 adsorption isotherms and pore development for these five samples are shown in Fig.5 and Table 2, respectively. According to the IUPAC classification, all adsorption isotherms belong to Type Ⅰ isotherm, it can be seen that the samples were predominated by micropores with a relatively small external surface. The nitrogen uptake was only significant in the low pressure range, *i e*, at relative pressures less than 0.1. In the high-pressure range, no further adsorption was observed and therefore the adsorption curve had reached equilibrium.

Compared with WAC, N_2 cumulative adsorption amount of MWAC decreases due to active components occupation. When the PH_3 adsorption curve has reached breakthrough, N_2 adsorption amount of MWAC-AB decreases sharply to 34.79 cm^3/g and the BET surface area is only 90 m^2/g. Once the PH_3 adsorption curve has reached equilibrium, N_2 adsorption amount and BET surface area of MWAC-AQ are almost zero. However, after undergoing 5 adsorption-regeneration cycles, N_2 adsorption amount and BET surface area of MWAC-R5 were recovered and almost equal to that of MWAC sample. This was because most of the sample pores after adsorption were occupied by adsorbed species. When regeneration process finished, the adsorbed species removed completely by water washing and therefore the BET surface area together with pore volume of MWAC-R5 could be increased to that of the fresh MWAC sample, which illustrated that this regeneration process was a cost-effective method. At the same time, N_2 adsorption isotherm of MWAC-R5 showed that the adsorption process was not a physical adsorption because PH_3 solubility in water was relatively low.

3.4.2 SEM/EDS analysis

SEM/EDS characterization results of the five samples are shown in Fig.6 and Table 3, respectively. For the WAC (Fig.6(a)), the surface was quite smooth and consists of 100% carbon element. Small pores, transitional pores, and large pores of different shapes are shown in this micrograph. Besides the same features with WAC micrograph, the white granular materials over the MWAC adsorbent (Fig.6(b)) were probably due to the presence of active components, being consistent with the results of EDS element analysis (39.02% of copper element). During adsorption, macro and mesopores allow rapid transport of the adsorbate into the interior of the carbon for subsequent diffusion into the micropore volume. Consequently, a well-developed porous network in all pore size ranges results in improved adsorption properties of the carbon[29].

It was observed that the MWAC-AB sample surface was irregular with the spherical and acicular aggregate materials because of the formation of adsorption species as shown in Fig.6(c). According to EDS analysis, 16.83% of phosphorus element existed in the MWAC-AB sample and oxygen element increased

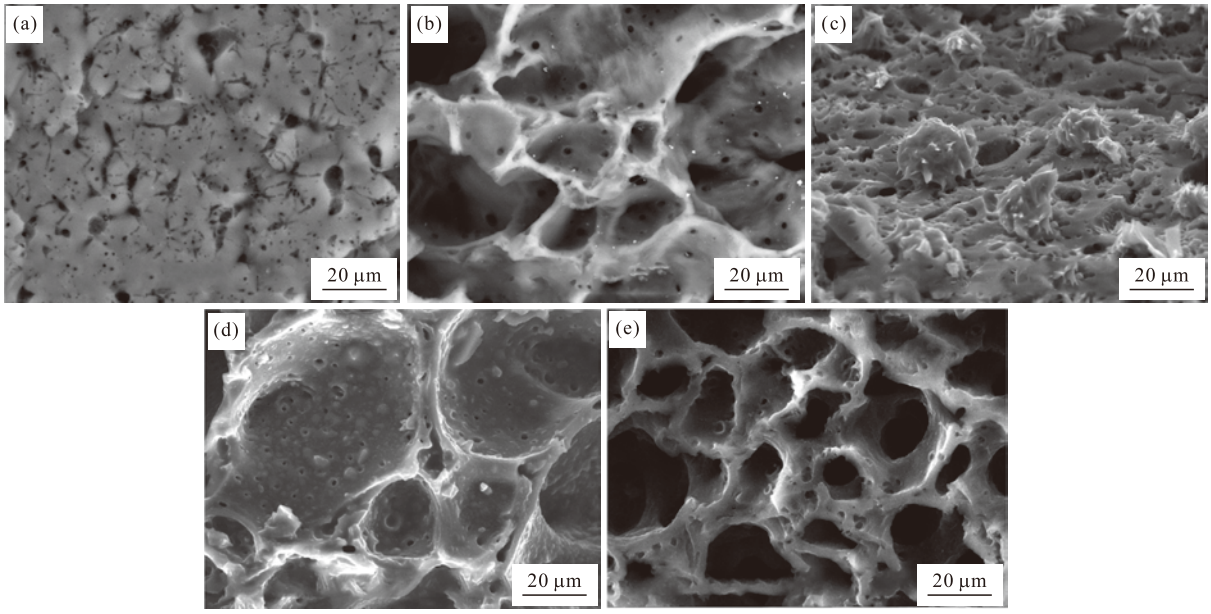

Fig.6 SEM characterizations of five different samples: (a) WAC, (b) MWAC, (c) MWAC-AB, (d) MWAC-AQ, (e) MWAC-R5

from 19.12% to 30.62%, which showed that adsorption species may be phosphorus oxides. As for the MWAC-AQ sample (Fig.6(d)), the pores were fully filled with adsorption species, without any pores except for some occasional cracks. Moreover, content of phosphorus element increased to 24.18%. After regeneration using water washing and air drying, the adsorption species disappear, giving rise to a pure pore structure as shown in Fig.6(e). Small pores, transitional pores, and large pores of different shapes are shown again in this micrograph. On the other hand, contents of phosphorus element and oxygen element decreased sharply. The result shows that this regeneration method provides an effective way for both adsorption species recycling and regeneration of exhausted carbons.

Table 3 EDS analysis of five different samples

Samples	Element analysis/wt%					
	C	O	Cu	Zn	La	P
WAC	100	0	0	0	0	0
MWAC	37.92	19.12	39.02	3	0.94	0
MWAC-AB	50.00	30.62	2.55	0	0	16.83
MWAC-AQ	51.10	22.20	2.52	0	0	24.18
MWAC-R5	89.44	5.66	2.04	0	0	2.86

3.4.3 XPS analysis

In order to clarify the valence state of Cu and P species on these five different samples, they were examined by XPS. Atom contents of these five different samples are illustrated in Table 4. The states of Cu species in these samples are evaluated by deconvolution of the Cu 2p region spectra using multiple Gaussian fitting functions, as shown in Table 5. The states of P species in the MWAC-AB and MWAC-AQ samples are illustrated in Table 6.

Compared with WAC samples, Cu species existed in MWAC samples, being consistent with SEM/EDS result. The main peak of Cu 2p in the range 933.43-935.78 eV and an accompanying shake-up satellite peak at 953.08-955.44 eV were assigned to Cu^{2+} species of CuO[15,30,31], indicating that Cu species existed in MWAC samples were CuO. Undergoing phosphine adsorption process, CuO species in MWAC-A samples disappeared due to the adsorption species deposition. Our previous articles[15,24] showed that PH_3 adsorption capacity on fresh AC without copper modification was rather low even if oxygen gas existed in the flowing mixed gas. However, the PH_3 removal efficiency on the AC modified by copper oxides increased significantly. There is a good possibility that CuO loaded onto the MWAC sample play an oxygen carrier role in the PH_3 adsorption-oxidation process. The following XPS analysis will demonstrate this discussion.

As shown in Tables 4 and 6, when the adsorption process has reached equilibrium, both O species and P species increase from 29.10% to 53.37% and from 3.92% to 14.04%, respectively, indicating that P species may transform to phosphorus oxides. On the other hand, the P 2p peak centered at 134.28-134.70 eV indicated that the presence of H_3PO_4 and the P 2p peak centered at 135.62-136.06 eV meanwhile, indicated the presence of $P_4O_{10}(P_2O_5)$[5,15,31]. The H_3PO_4 and P_4O_{10} species existed in MWAC-A samples were generated by the PH_3 adsorption-oxidation process. Fresh MWAC had no phosphorus species. After adsorption

breakthrough, it was observed that the relative percentage of H_3PO_4 (67.08%) was more than that of P_4O_{10} (32.92%). Arriving adsorption equilibrium, the relative percentage of H_3PO_4 increased to 75.28%, which indicating that part of P_4O_{10} were converted to H_3PO_4 in the presence of water. The result also demonstrates that CuO loaded on the MWAC sample play an oxygen carrier role in the adsorption process. In this process, the MWAC firstly adsorbs PH_3 and then PH_3 adsorbed on the MWAC can be oxidized to form H_3PO_4 and P_2O_5 in the presence of oxygen gas.

Table 4 XPS analysis of five different samples

Samples	Atom content/%					
	C1s	O1s	Cu2p	P2p	Zn2p	La2p
WAC	75.65	24.35	0	0	0	0
MWAC	75.35	22.60	2.05	0	0	0
MWAC-AB	66.98	29.10	0	3.92	0	0
MWAC-AQ	32.59	53.37	0	14.04	0	0
MWAC-R5	83.05	16.91	0	0	0	0

Table 5 Composition of the Cu2p peak for MWAC

Element	Band No.	Binding energy/eV	Peak area ratio /%	Chemical speciation
Cu2p	1	933.43	41.28	CuO
	2	935.78	21.88	CuO
	3	953.08	22.00	satellite peaks of CuO
	4	955.44	14.84	satellite peaks of CuO

Table 6 Composition of the P2p peak for MWAC-AB and MWAC-AQ

Samples	Element	Band No.	Binding energy/eV	Peak area ratio/%	Chemical speciation
MWAC-AB	P2p	1	134.28	67.08	H_3PO_4
		2	135.62	32.92	P_4O_{10}
MWAC-AQ	P2p	1	134.70	75.28	H_3PO_4
		2	136.06	24.72	P_4O_{10}

3.4.4 FTIR analysis

Infrared spectroscopy provides information on the chemical structure of the adsorbent material. Fig.7 shows FTIR spectra of five different samples. In the range of 4 000-1 380 cm^{-1}, these absorption bands belong to all five samples and these surface functional groups are important characteristics of activated carbons. The band at 1 115 cm^{-1} for the MWAC is attributed to the C-O stretching vibration of various functional groups. Compared with the MWAC sample, theses absorption bands of the MWAC-AB and MWAC-AQ samples peak at about 1 220, 1 169, and 1 000 cm^{-1}. Moreover, the absorption bands of the MWAC-AQ sample are more intense than that of the MWAC-AB sample. Therefore, it is necessary to identify these absorption bands in order to analyze PH_3 adsorption mechanism. According to Chapman *et al*[32], Stefov *et al*[33] and our previous work[15], the absorption bands at about 1 220 cm^{-1} of MWAC-AB and MWAC-AQ samples were ascribed to P-O-H in-plane bending vibration of H_3PO_4. The absorption bands at about 1 169 and 1 000 cm^{-1} of MWAC-AB and MWAC-AQ samples were characteristic to antisymmetric stretching vibration (v_3) of PO_4^{3-}. The FTIR absorption band differences among these five samples showed that PH_3 adsorbed on the MWAC sample would be oxidized to form H_3PO_4 in the presence of oxygen gas and the oxidized products were adsorbed onto activated carbon more easily than PH_3.

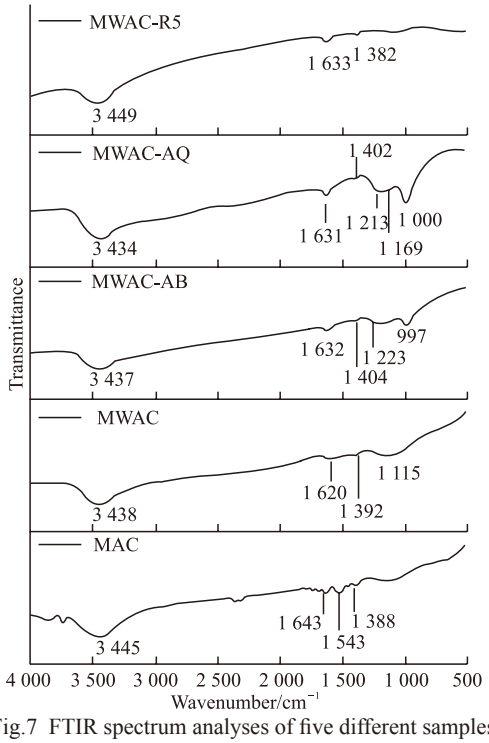

Fig.7 FTIR spectrum analyses of five different samples

3.4.5 Adsorption mechanism analysis

According to the above experimental results and characterizations, PH_3 adsorption mechanism analysis over the MWAC adsorbent is as follows.

Both PH_3 adsorption isotherms and adsorption thermodynamics show that phosphine adsorption onto the MWAC adsorbent is mainly chemical adsorption. There is an optimal adsorption temperature of 343K and values of isosteric heat of adsorption range from 43 kJ/mol to 90 kJ/mol. This is generally consistent with

the regeneration results shown in Fig.3. The exhausted adsorbents can be regenerated to about 91% of PH_3 breakthrough adsorption capacity and time of the fresh MWAC adsorbent. Because PH_3 solubility in water is relatively low, PH_3 adsorbed on the adsorbent may be oxidized to form H_3PO_4 and P_2O_5, which are removed easily from its surface when using water washing regeneration.

According to thermodynamical equilibrium analysis calculated by Factsage 6.0[22], when the molar ratio of O_2 to PH_3 in mixed fluent is not less than 2, PH_3 will react with oxygen to form H_3PO_4 and only a little $(P_2O_5)_2$. However, in practical experimental process, the PH_3 removal efficiency is almost equal to zero when active components do not exist in the adsorbent, which indicating that CuO loaded onto the MWAC sample may play an oxygen carrier role in the PH_3 adsorption-oxidation process. All characterization results are also consistent with this conclusion.

After regeneration, the adsorption species disappeared, giving rise to a pure pore structure as shown in Fig.5(e). It also observes that BET surface area and pore volume of MWAC-R5 can be increased to that of the fresh sample in N_2 adsorption isotherm analysis, being consistent with the XPS and FTIR characterizations. As shown in Tables 4-6, fresh MWAC has no phosphorus species. After adsorption, the H_3PO_4 and P_4O_{10} species existed in MWAC-A samples are generated by the PH_3 adsorption-oxidation process. On the other hand, the FTIR absorption band differences among these five different samples probably show that PH_3 adsorbed on the MWAC sample can be oxidized to form H_3PO_4 in the presence of oxygen gas and the oxidization products are adsorbed onto activated carbon more easily than PH_3.

The above results provide a good basis for proposing a possible mechanism for the formation of H_3PO_4 and P_2O_5. The lattice oxygen in copper oxides is clearly involved in the reaction. Possible reaction steps are proposed as follows:

$$PH_3 + X \rightleftharpoons PH_3\text{-}X \quad (3)$$

$$O_2 + X \rightleftharpoons O_2\text{-}X \quad (4)$$

$$PH_3\text{-}X + 4OM \rightleftharpoons H_3PO_4\text{-}X + 4M \quad (5)$$

$$4PH_3\text{-}X + 16OM \rightleftharpoons (P_2O_5)_2\text{-}X + 6H_2O + 16M \quad (6)$$

$$(P_2O_5)_2\text{-}X + 6H_2O \rightleftharpoons 4H_3PO_4\text{-}X \quad (7)$$

$$2M + O_2\text{-}X \rightleftharpoons 2OM + X \quad (8)$$

The PH_3 adsorption-oxidation begins with physical adsorption of PH_3 and O_2 over the active point of MWAC adsorbent (Eqs.(3) and (4)). Because PH_3 physical adsorption amount is small, PH_3 adsorbed on the active point reacts rapidly with lattice oxygen of active components to form H_3PO_4 and P_2O_5 (Eqs.(5) and (6)), indicating that PH_3 and O_2 physical adsorption process is the very important step. Subsequently, P_2O_5 can also react with water to form H_3PO_4 (Eq.(7)). The formed H_3PO_4 and P_2O_5 adsorb onto the active point of active components. Simultaneously, lattice oxygen of active components is supplied by O_2 adsorbed (equation 8). According to the Reduction-Oxidation (Redox) mode, Oxygen used for PH_3 oxidation reaction does not come from O_2 in mixed gas but from lattice oxygen of active components. The exhausted lattice oxygen is supplied by oxygen adsorbed on the MWAC adsorbent and then the reduced active components are oxidized to the initial state. Moreover, the oxidation species are H_3PO_4 and P_2O_5. Therefore, the high removal efficiency and big equilibrium adsorption capacity for PH_3 adsorption are related to the large surface area and high oxidation activity of the MWAC adsorbent in PH_3 adsorption-oxidation to H_3PO_4 and P_2O_5. There are two reasons why PH_3 removal efficiency decreased. Firstly, the MWAC pores were fully filled with adsorption species (H_3PO_4 and P_2O_5) and there was no pore for adsorption species filling. Secondly, the active components were surrounded by adsorption species and lattice oxygen of active components cannot be supplied by O_2 in mixed gas, which resulting in chemical adsorption interruption.

4 Conclusions

MWAC adsorbent would be one of the candidates for both PH_3 adsorption removal and phosphorus recycling from yellow phosphorus tail gas. The maximum PH_3 equilibrium adsorption capacity was 595.56 mg/g at the optimal adsorption temperature of 343 K. The regeneration method using water washing and air drying provided an effective way for both adsorption species recycling and regeneration of exhausted carbons. The high removal efficiency and big equilibrium adsorption capacity for PH_3 adsorption were related to the large surface area and high oxidation activity of the MWAC adsorbent in PH_3 adsorption-oxidation to H_3PO_4 and P_2O_5. Moreover, a possible

mechanism for PH_3 adsorption removal was proposed.

References

[1] Ning P, Wang XY. Advanced Purification and Comprehensive Utilization of Yellow Phosphorous off Gas[J]. *Frontiers of Environmental Science & Engineering*, 2015, 9(2): 181-189

[2] Ma LP, Ning P, Zhang YY, *et al.* Experimental and Modeling of Fixed-bed Reactor for Yellow Phosphorous Tail Gas Purification over Impregnated Activated Carbon[J]. *Chemical Engineering Journal*, 2008, 137(3): 471-479

[3] Ning P, Yi HH, Yu QF, *et al.* Effect of Zinc and Cerium Addition on Property of Copper-based Adsorbents for Phosphine Adsorption[J]. *Journal of Rare Earths*, 2010, 28(4): 581-586

[4] Yu QF, Tang XL, Yi HH, *et al.* Equilibrium and Heat of Adsorption of Phosphine on $CaCl_2$-Modified Molecular Sieve[J]. *Asia-Pacific Journal of Chemical Engineering*, 2009, 4(5): 612-617

[5] Wang XQ, Ning P, Shi Y, *et al*. Adsorption of Low Concentration Phosphine in Yellow Phosphorus off-gas by Impregnated Activated Carbon[J]. *Journal of Hazardous Materials*, 2009, 171(1-3): 588-593

[6] Yu QF, Li M, Ning P, *et al.* Preparation and Phosphine Adsorption of Activated Carbon Prepared from Walnut Shells by KOH Chemical Activation[J]. *Separation Science and Technology*, 2014, 49(15): 2 366-2 375

[7] Ren ZD, Quan SS, Zhu YC, *et al.* Purification of Yellow Phosphorus Tail Gas for the Removal of PH_3 on the Spot with Flower-shaped CuO/AC[J]. *Rsc Advances*, 2015, 5(38): 29 734-29 740

[8] Yang LP, Yi HH, Tang XL, *et al.* Effect of Rare Earth Addition on Cu-Fe/AC Adsorbents for Phosphine Adsorption from Yellow Phosphorous Tail Gas[J]. *Journal of Rare Earths*, 2010, 28(0): 322-325

[9] Elliot B, Balma F, Johnson F. Exhaust Gas Incineration and the Combustion of Arsine and Phosphine[J]. *Solid State Technology*, 1990, 33(1): 89-92

[10] Herman T, Soden S. Efficieny Handling Effluent Gases through Chemical Scrubbing[C]. *AIP Conference Proceedings*, 1988, 166(1): 99-108

[11] Li JY, Ning P, Qu GF. Research on the Cu(II)-Co(II) Catalyzed Oxidation of Phosphine in Aqueous Solution[J]. *Journal of Wuhan University Technology*, 2007, 29(10):63-65, 69

[12] Colabella JM, Stall RA, Sorenson CT. The Adsorption and Subsequent Oxidation of AsH_3 and PH_3 on Activated Carbon[J]. *Journal of Crystal Growth*, 1988, 92: 189-195

[13] Hsu JN, Tsai CJ, Chiang C, *et al.* Silane Removal at Ambient Temperature by Using Alumina-supported Metal Oxide Adsorbents[J]. *Journal of the Air & Waste Management Association*, 2007, 57(2): 204-210

[14] Ning P, Bart H-J, Wang XQ, *et al.* Removal of P_4, PH_3 and H_2S from Yellow Phosphorus Tail Gas by a Catalytic Oxidation Process[J]. *Engineering Science*, 2005, 7(6): 27-35

[15] Yi HH, Yu QF, Tang XL, *et al.* Phosphine Adsorption Removal from Yellow Phosphorus Tail Gas over CuO-ZnO-La_2O_3/Activated Carbon[J]. *Industrial & Engineering Chemistry Research*, 2011, 50(7): 3 960-3 965

[16] Bhatnagar A, Sillanpaa M. Utilization of Agro-industrial and Municipal Waste Materials as Potential Adsorbents for Water Treatment-A Review[J]. *Chemical Engineering Journal*, 2010, 157(2-3): 277-296

[17] Yorgun S, Yıldız D. Preparation and Characterization of Activated Carbons from Paulownia Wood by Chemical Activation with H_3PO_4[J]. *Journal of the Taiwan Institute of Chemical Engineers*, 2015, 53: 122-131

[18] Yu QF, Li M, Ji X, *et al.* Characterization and Methanol Adsorption of Walnut-shell Activated Carbon Prepared by KOH Activation[J]. *Journal of Wuhan University of Technology-Material Science Edition*, 2016;31(2): 260-268

[19] Nowicki P, Pietrzak R, Wachowska H. Sorption Properties of Active Carbons Obtained from Walnut Shells by Chemical and Physical Activation[J]. *Catalysis Today*, 2010, 150(1-2): 107-114

[20] Yang J, Qiu KQ. Preparation of Activated Carbons from Walnut Shells via Vacuum Chemical Activation and Their Application for Methylene Blue Removal[J]. *Chemical Engineering Journal*, 2010, 165(1): 209-217

[21] Gu X, Su Z, Xi H. New Activated Carbon with High Thermal Conductivity and Its Microwave Regeneration Performance[J]. *Journal of Wuhan University of Technology- Material Science Edition*, 2016, 31(2): 328-333

[22] Yu QF. Adsorbent Preparation and Adsorption Mechanism Research for Low Concentration PH_3 Adsorption Removal[D]. *Kunming: Kunming University of Science & Technology*, 2011

[23] Yu QF, Yi HH, Tang XL, *et al.* Adsorption and Prediction of Adsorption Isotherm onto Activated Carbon[J]. *Journal of Wuhan University Technology*, 2010;32(1): 34-37

[24] Yu QF, Ning P, Yi HH, *et al.* Effect of Preparation Conditions on the Property Cu/AC Adsorbents for Phosphine Adsorption[J]. *Separation Science and Technology*, 2012, 47: 527-533

[25] Li S, Hao JM, Ning P, *et al.* Preparation of Cu-Fe Nanocomposites Loaded Diatomite and Their Excellent Performance in Simultaneous Adsorption/oxidation of Hydrogen Sulfide and Phosphine at Low Temperature[J]. *Separation and Purification Technology*, 2017, 180(1): 23-35

[26] Xu XW, Huang GQ, Qi S. Properties of AC and 13X Zeolite Modified with $CuCl_2$ and $Cu(NO_3)_2$ in Phosphine Removal and the Adsorptive Mechanisms[J]. *Chemical Engineering Journal*, 2017, 316: 563-72

[27] Rothstein DP, Wu B-G, Lee TV, *et al*. Adsorption Isotherms and Isosteric Heats of Adsorption for Ethane, Propane, and N-butane on Polystyrene[J]. *Journal of Colloid and Interface Science*, 1985, 106(2): 399-409

[28] Hill T. Statistical Mechanics of Adsorption. V. Thermodynamics and Heat of Adsorption[J]. *The Journal of Chemical Physics*, 1949, 17: 520-535

[29] Martinez M, Torres M, Guzman C, *et al.* Preparation and Characteristics of Activated Carbon from Olive Stones and Walnut Shells[J]. *Industrial Crops and Products*, 2006, 23(1): 23-28

[30] ZahmakIran M, zkar S, Kodaira T, *et al.* A Novel, Simple, Organic Free Preparation and Characterization of Water Dispersible Photoluminescent Cu_2O Nanocubes[J]. *Materials Letters*, 2009, 63(3-4): 400-402

[31] Moulder J, Chastain J. *Handbook of X-ray Photoelectron Spectroscopy*[M]. Perkin-Elmer Eden Prairie, MN, 1992

[32] Chapman A, Thirlwell L. Spectra of Phosphorus Compounds--I the Infra-red Spectra of Orthophosphates[J]. *Spectrochimica Acta*, 1964, 20(6): 937-947

[33] Stefov V. Infrared and Raman Spectra of Magnesium Ammonium Phosphate Hexahydrate (Struvite) and Its Isomorphous Analogues. I. Spectra of Protiated and Partially Deuterated Magnesium Potassium Phosphate Hexahydrate[J]. *Journal of Molecular Structure*, 2004, 689(1-2): 1-10